



# COMPARISON OF FREQUENCY RESPONSE AND PERTURBATION METHODS TO EXTRACT LINEAR MODELS FROM A NONLINEAR SIMULATION

Keith A. Balderson

Jeffrey T. Weathers

Naval Air Warfare Center, Patuxent River, Maryland

1994

## Abstract

The purpose of this paper is to compare two distinct methods to extract a linear state-space model about a reference flight condition from a nonlinear simulation. The frequency response method uses a time history input which contains the frequencies of interest to drive the simulation. The frequency input and the output of the simulation are transformed to the frequency domain, and the desired frequency responses of the simulation are calculated. A linear model is then fit to the frequency responses using system identification techniques. The perturbation method extracts a linear model by perturbing the model states and inputs from the reference flight condition and calculating the resulting model coefficients. Both methods were used to extract a fourth order longitudinal state-space model from the V-22 full nonlinear simulation. The time history responses and system matrices of the extracted models were compared. The comparison showed that both methods are effective means to reduce a nonlinear simulation to a linear state-space model.

## Nomenclature

$a_x$	x body axis acceleration (ft/sec <sup>2</sup> )
$a_z$	z body axis acceleration (ft/sec <sup>2</sup> )
A	State-space system matrix
B	State-space control matrix
C	State-space output matrix
$C_{xy}$	Coherence function
D	State-space output control matrix
$F_1$	Chirp-z transform starting frequency (rad/sec)

$F_2$	Chirp-z transform ending frequency (rad/sec)
H	Transfer function
$L_w$	Length of windows
$L_{ssw}$	Length of sum of sine waves signal
$N_w$	Number of windows
$P_{xx}$	Input power spectral density (dB)
$P_{xy}$	Input-output cross spectral density (dB)
$P_{yy}$	Output power spectral density (dB)
qb	pitch rate (deg/sec)
t	Time (seconds)
u	State-space input vector
ub	x body axis velocity (ft/sec)
wb	z body axis velocity (ft/sec)
x	State-space state vector
X	Input signal Fourier Coefficients
y	State-space output vector
Y	Output signal Fourier Coefficients
$\delta_e$	Elevator position (deg)
$\delta_{lon}$	Longitudinal stick position (in)
$\Delta t$	Simulation time step (sec)
$\Delta\omega_{czt}$	Chirp-z transform frequency resolution (rad/sec)
$\Delta\omega_{ssw}$	Sum of sine waves signal frequency resolution (rad/sec)
$\lambda$	eigenvalue
$\Lambda$	dynamic mode
$\omega$	Frequency (rad/sec)
$\theta$	Pitch attitude (deg)
*	Denotes complex conjugate

## Introduction

Modern aircraft simulators must represent highly nonlinear vehicle aerodynamics to provide effective pilot training and accurate engineering analysis. However, it is still useful to obtain linear

94 9 01 201

DTIC QUALITY INSPECTED 1

DISTRIBUTION STATEMENT A  
Approved for public release  
Distribution Unlimited

94-28642



1498

TO WHOM IT MAY CONCERN:

Here is a copy of Professional Papers written by various people here at the Naval Air Warfare Center Aircraft Division. It was requested that a copy of each of the professional papers be sent to DTIC for retention.

If you have any questions, please contact Dorothy Reppel, 326-1709 or (301) 826-1709.

P.S. All the enclosed papers have been cleared for public release.

<b>Accession For</b>	
NTIS GRA&I	<input checked="checked" type="checkbox"/>
DTIC TAB	<input type="checkbox"/>
Unannounced	<input type="checkbox"/>
Justification	
By	
Distribution/	
Availability Codes	
Dist	Avail and/or Special
A-1	

aerodynamic models about a reference flight condition to take advantage of powerful linear theory techniques, especially for control law analysis and specification compliance.

The Naval Air Warfare Center's Manned Flight Simulator (MFS) has developed a highly modular simulation architecture. The Controls Analysis and Simulation Test Loop Environment (CASTLE) is a generic shell structure designed for simulation development, execution, and analysis.

One of the CASTLE facilities for engineering analysis is the MANeuver GENERator (MANGEN). The MANGEN facility can be used with an input data file to overdrive any desired simulation control. Another of the CASTLE facilities is the Linear Model Extraction (LME) program. LME is used to generate a linear state-space model using the offset derivative method.

The V-22 tilt-rotor simulation under the CASTLE architecture was run in non-realtime mode to produce the simulation data for the linear model comparisons. MANGEN was used to overdrive the control input for the frequency response method, and LME was used to extract the linear model for the perturbation method.

### V-22 Simulation Overview

The V-22 Osprey is a tilt-rotor aircraft capable of flight from hover to high speed airplane mode. Control of the V-22 is accomplished through both conventional airplane and helicopter controls. The airplane controls include elevator, rudders and flaperons, and the helicopter controls include longitudinal cyclic, lateral cyclic, and collective pitch.

The V-22 has a digital fly-by-wire control system consisting of a primary flight control system (PFCS) and an automatic flight control

system (AFCS). The PFCS provides pilot shaping and essential feedback loops for primary control. The AFCS is designed to provide level 1 handling qualities and auto-pilot functions.

The V-22 simulation at the MFS is a high fidelity full envelope simulation utilized for pilot training and engineering analysis. The airframe model is based on Bell Helicopter's Generic Tilt-Rotor Simulation.

### Initial Conditions

The simulation initial flight conditions were; level steady state flight, nacelles fixed in airplane mode, true velocity of 200 knots, and constant flap setting. The rotor speed and flapping controllers were disabled in the PFCS to maintain constant swashplate positions. The core AFCS functions were active. Longitudinally, this provides a pitch attitude command system with pitch attitude and pitch rate feedback in the longitudinal stick to elevator path.

### Perturbation Method

The Linear Model Extraction (LME) facility under the CASTLE architecture is capable of obtaining linear models from the non-linear simulation, in the standard state-space form:

$$\dot{x} = Ax + Bu$$

$$y = Cx + Du$$

where

$$A = \begin{bmatrix} \frac{\partial \dot{x}_1}{\partial x_1} & \frac{\partial \dot{x}_1}{\partial x_2} & \dots \\ \frac{\partial \dot{x}_2}{\partial x_1} & \frac{\partial \dot{x}_2}{\partial x_2} & \dots \\ \vdots & \vdots & \ddots \end{bmatrix} \quad B = \begin{bmatrix} \frac{\partial \dot{x}_1}{\partial u_1} & \frac{\partial \dot{x}_1}{\partial u_2} & \dots \\ \frac{\partial \dot{x}_2}{\partial u_1} & \frac{\partial \dot{x}_2}{\partial u_2} & \dots \\ \vdots & \vdots & \ddots \end{bmatrix}$$

$$C = \begin{bmatrix} \frac{\partial y_1}{\partial x_1} & \frac{\partial y_1}{\partial x_2} & \dots \\ \frac{\partial y_2}{\partial x_1} & \frac{\partial y_2}{\partial x_2} & \dots \\ \vdots & \vdots & \ddots \end{bmatrix} \quad D = \begin{bmatrix} \frac{\partial y_1}{\partial u_1} & \frac{\partial y_1}{\partial u_2} & \dots \\ \frac{\partial y_2}{\partial u_1} & \frac{\partial y_2}{\partial u_2} & \dots \\ \vdots & \vdots & \ddots \end{bmatrix}$$

The user supplies LME with the states, state derivatives, inputs and outputs of the model to be extracted, as well as perturbation sizes of the states and inputs. LME uses the offset derivative method for extracting the linear models. In this method, biases are added to each input and state, and the resulting changes in outputs and state derivatives are recorded. Integration is frozen within the simulation during LME so that the state derivatives are not allowed to propagate. A schematic of this process is shown in figure 1.

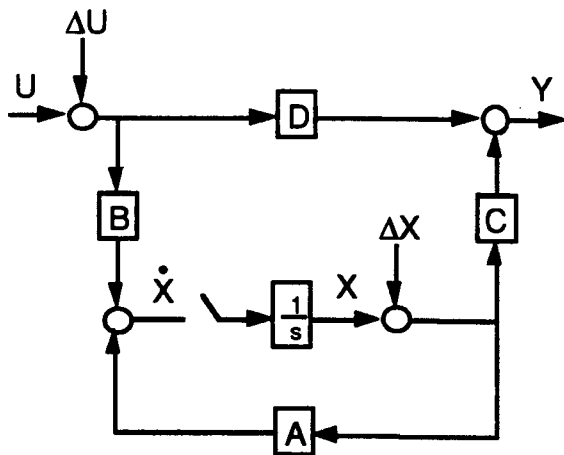


Figure 1. LME Schematic

The state-space matrices are then computed as:

$$A_{ij} = \frac{\Delta \dot{x}_i}{\Delta x_j} \quad B_{ik} = \frac{\Delta \dot{x}_i}{\Delta u_k}$$

$$C_{nj} = \frac{\Delta y_n}{\Delta x_j} \quad D_{nk} = \frac{\Delta y_n}{\Delta u_k}$$

Since the simulation is nonlinear, the change in outputs and state derivatives for different size perturbations will not be perfectly linear. The user specifies four perturbation sizes for each input and state. LME perturbs the simulation positively and negatively for each of the perturbation sizes and picks the perturbation size that results in the best linearity. A typical example of the perturbation selection is shown in figure 2.

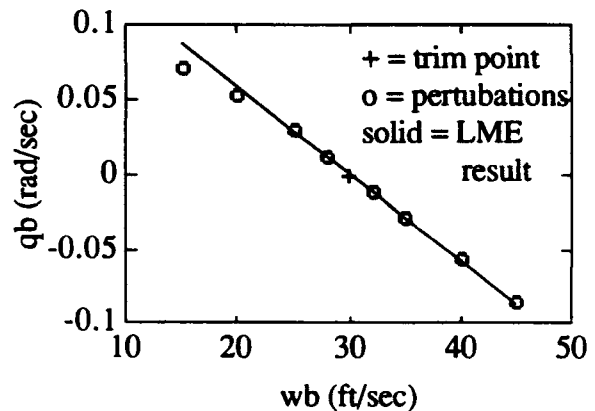


Figure 2. LME Perturbation Selection

The output of LME is the state-space model as well as information describing the linearity of each coefficient.

#### Model Definition

The input to the model was elevator position and the outputs were pitch rate and normal acceleration. The states chosen to represent the aircraft dynamics were:

x body velocity  
 y body velocity  
 z body velocity  
 roll rate  
 pitch rate  
 yaw rate  
 roll attitude  
 pitch attitude  
 heading angle  
 altitude

Since the rotors contribute significantly to the total dynamics, the following states were included.

left longitudinal flapping angle  
 right longitudinal flapping angle  
 left lateral flapping angle  
 right lateral flapping angle  
 rotor speed  
 right gas generator speed  
 left gas generator speed

The resulting model has one input,

two outputs and seventeen states.

### Model Reduction

High order linear models are necessary for accurate analysis of control systems. Low order models are often desired for design of control systems and analysis of flying qualities. In this case, a fourth order model representing only the longitudinal dynamics was desired.

Some of the states in the extracted model represent off-axis responses and contribute little, if any, to the longitudinal dynamics. The states corresponding to the rotor dynamics, however, affect both the phugoid and short period. These effects need to be included in the reduced order model.

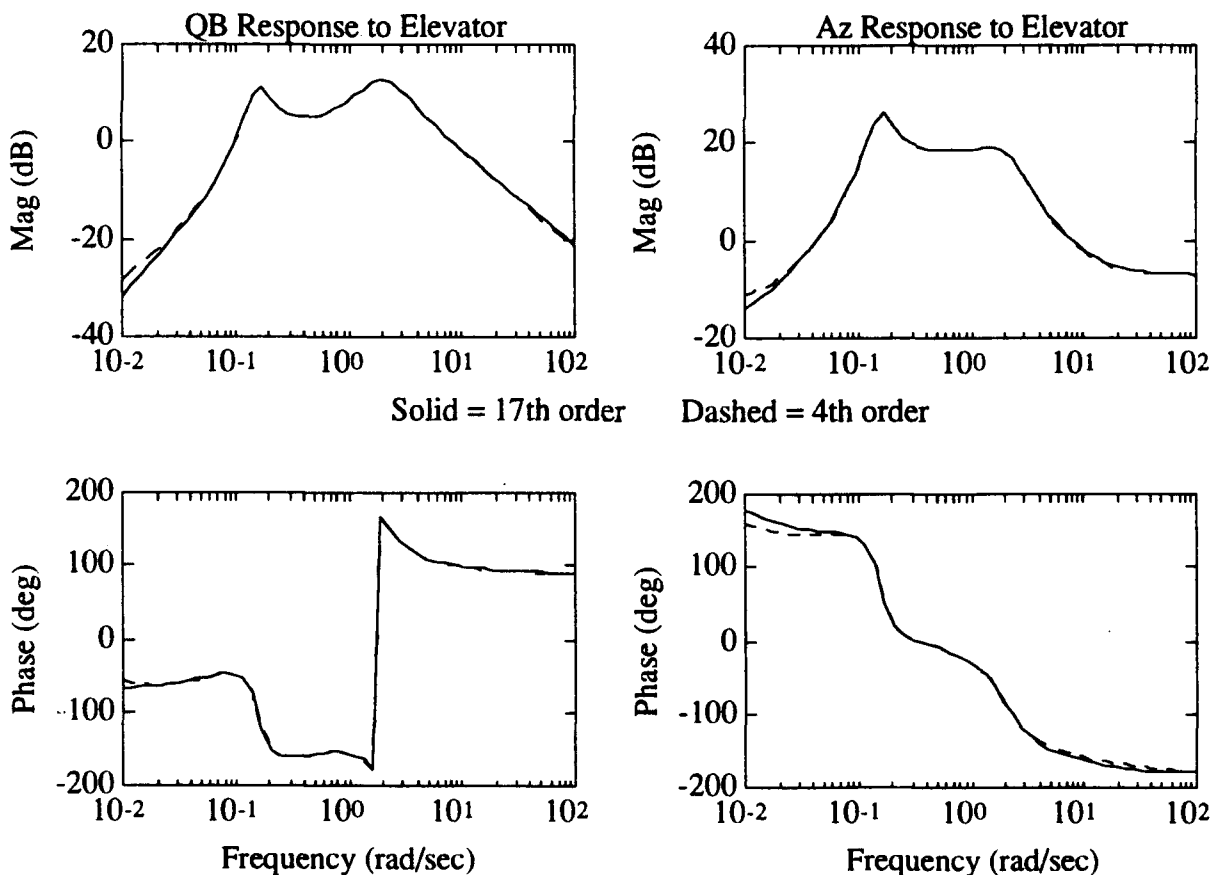


**Figure 3.** Model Reduction Results

The model reduction method chosen for this case was the modal truncation method. Modal truncation involves transforming the model into modal form:

$$\dot{x} = \begin{bmatrix} \Lambda_1 & 0 \\ 0 & \Lambda_2 \end{bmatrix} x + B_m u$$

$$y = C_m x + D_m u$$

where  $\Lambda$  is a mode of the system. For a first order mode,  $\Lambda$  is equal to the eigenvalue ( $\lambda$ ). A second order mode is represented as:

$$\Lambda = \begin{bmatrix} \text{real}(\lambda) & \text{imag}(\lambda) \\ -\text{imag}(\lambda) & \text{real}(\lambda) \end{bmatrix}$$

The contribution of each mode to the overall frequency response is calculated. The modes with the highest contribution are retained, the others are truncated.

The phugoid and short period were easily identified with the model in modal format. The four states corresponding to the phugoid and short period second order modes make up the reduced order model. The remaining eleven states were truncated. Figure 3 shows the results of the reduction.

### Frequency Response Method

#### Overview

The frequency response method uses a time history input which contains the frequencies of interest to drive the simulation. The frequency input and the output of the simulation are transformed to the frequency domain, and the desired frequency responses of the simulation are calculated. A linear model is then fit to the frequency responses using system identification techniques.

To extract a fourth order longitudinal model from the V-22 simulation, the longitudinal stick position was used as the input signal, and the desired frequency responses were the  $u_b$ ,  $w_b$ ,  $a_x$ ,  $a_z$ , and  $q_b$  responses to the elevator position. By using the longitudinal stick as the input (instead of directly driving the elevator position) the control system reduced excursions from the reference flight condition. Figure 4 is a simple schematic of the simulation process.

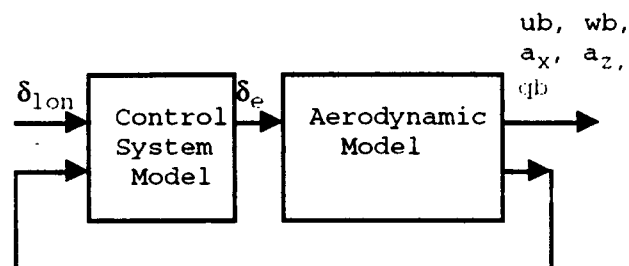


**Figure 4** Schematic of Simulation Process

#### Input Signal Selection

A variation of the swept sine input has been the dominant input design for frequency response calculations.<sup>1,2,3</sup> The design goals for the frequency input were to provide good spectral excitement in the frequency range of interest and to prevent the aircraft (or simulation) from straying too far away from the reference flight condition.

For non-realtime simulation without a pilot in the loop, a swept sine longitudinal stick input drove the V-22 simulation away from the reference flight condition, even with the AFCS engaged. Therefore, a new signal that prevented large excursions from the reference flight condition was designed using a sum of sine waves. To construct the new signal, alternating positive and negative sine waves at selected frequencies were summed into a single signal.

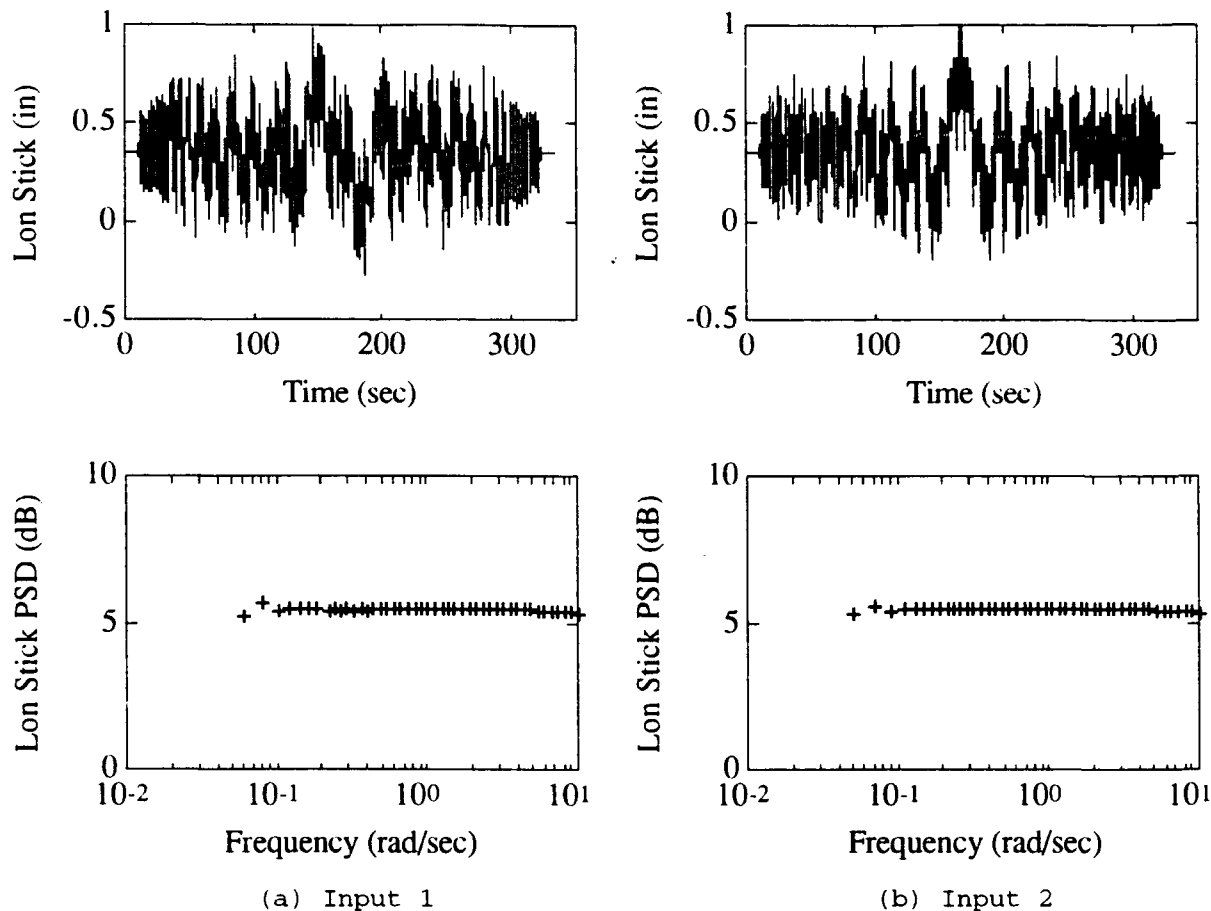


**Figure 5.** Sum of Sine Waves Longitudinal Stick Inputs

The sum of sines input proved superior to the swept sine input for two reasons. The low frequency input was applied throughout the entire signal (instead of only at the beginning) providing better low frequency spectral content, and the signal was easily designed to limit the excursions from the reference flight condition.

#### Input Signal Design

Two design parameters, the frequency resolution and the signal length, were considered when constructing the sum of sines input. To produce a signal that has equal power about the half-period, the signal length was determined from the input frequency resolution.

$$L_{SSW} = \frac{t}{\Delta t} = \frac{2\pi/\Delta\omega_{SSW}}{\Delta t}$$

A frequency resolution of 0.02 radians per second was selected to provide good low frequency excitation and to limit the simulation run time. Limiting the simulation run time reduced the number of data points to process for the frequency response calculation. The length of the sum of sines signal was calculated using a simulation time step of 0.0333333 seconds.

$$L_{SSW} = \frac{2\pi/0.02}{0.0333333} = 9425$$

To excite the V-22 fourth order longitudinal dynamics, a frequency range from 0.05 to 10 radians per

second was selected based on previous simulation data. The low frequency of 0.05 radians per second captured the phugoid dynamics, and the high frequency of 10 radians per second bounded the short period mode.

Two input signals were designed to produce data from two separate simulation runs. Input signal 1 contained 45 sine waves with frequencies selected from a vector of 0.06 to 10 radians per second. Input signal 2 contained 45 sine waves with frequencies selected from a vector of 0.05 to 9.9 radians per second. The frequency vectors for inputs 1 and 2 had a frequency resolution of 0.02 radians per second.

The frequencies used in the input signals were selected to be approximately evenly spaced on a logarithmic scale over the frequency range. However, not quite enough low frequencies were available in the frequency vector, and the resulting signals were slightly more heavily concentrated at higher frequencies.

After the sine waves were summed, the signals were zero padded at the beginning and end to create a total length of 10,000 points. The zero padding added reference flight data to the beginning and end of the simulation output.

Finally, the signals were appropriately scaled and biased for the reference longitudinal stick position. The resulting signals are shown in Figure 5. Notice from the power spectral densities the even power content at the discrete frequencies contained in the inputs.

#### Simulation Run

The V-22 simulation was initialized to the level flight, steady state reference condition, and the longitudinal stick inputs shown in Figure 5 were used to drive the simulation. Overdriving the longitudinal stick position with the

input data files was accomplished using the CASTLE MANGEN facility.

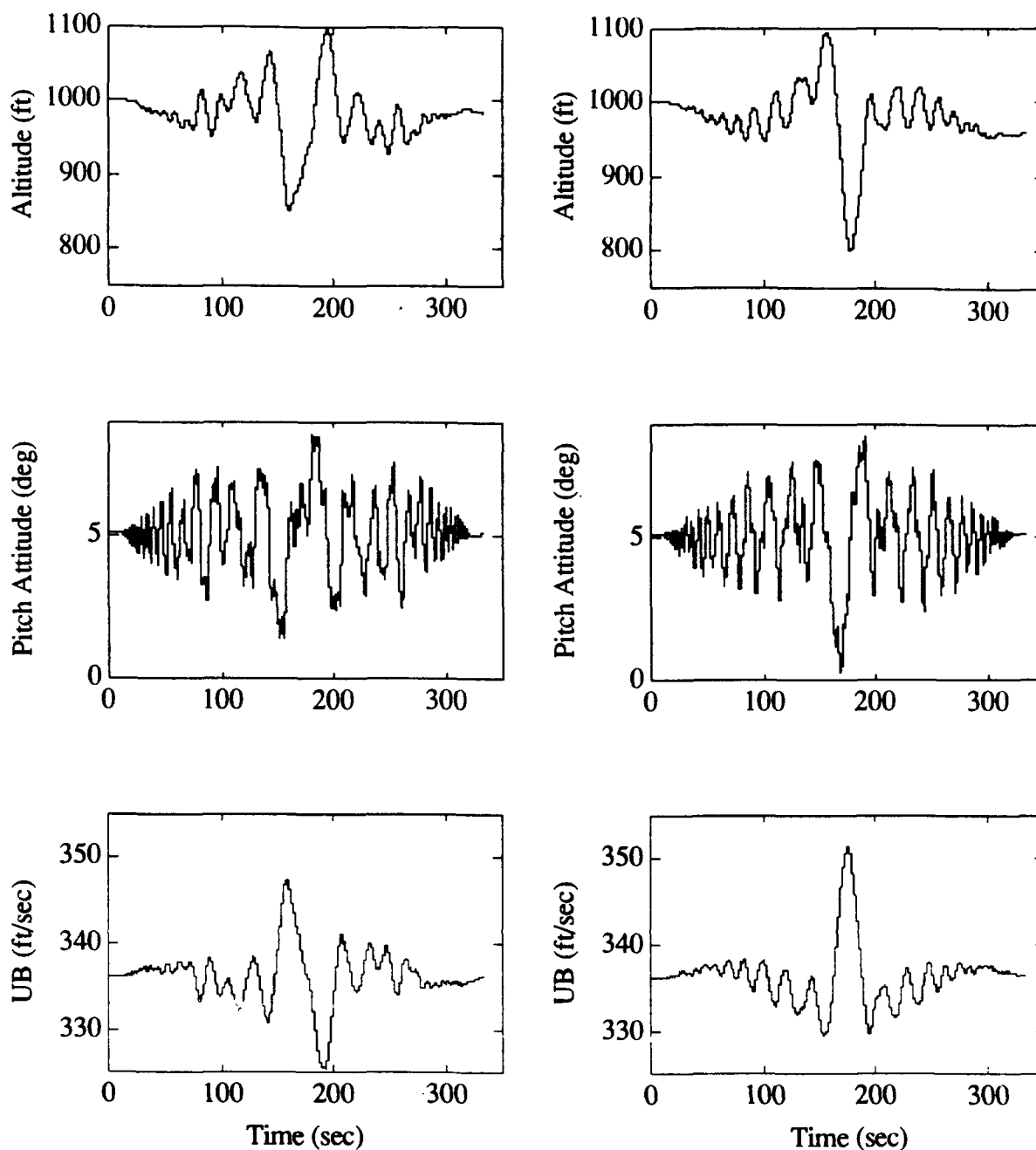
The altitude, pitch attitude and u body velocity time histories for simulation runs 1 and 2 are shown in Figure 6. Notice that the time histories end very near the reference flight condition even after a simulation run of more than five minutes.

#### Frequency Response Calculation

The process to calculate a frequency response from frequency sweep time history data is well defined.<sup>1,4,5</sup> The process is the same for a sum of sines input, except that only discrete frequencies are contained in the signal. Therefore, the simulation output contained spectral information only at the discrete frequencies included in the input. A frequency bookkeeping was maintained when processing the data to insure that only the discrete frequencies contained in the input were used to calculate the resulting frequency responses.

The  $u_b$ ,  $w_b$ ,  $a_x$ ,  $a_z$ ,  $q_b$ , and  $\delta_e$  time histories from simulation runs 1 and 2 were concatenated, and the data was detrended to remove the bias and linear drift. The concatenated data was windowed with two non-overlapping 10,000 point rectangular windows. Large window sizes give better low frequency resolution, and small window sizes average the data to reduce high frequency noise. Since the simulation time history data contained essentially no noise, minimal averaging was necessary.

The chirp z-transform was used to process the time history data. This advanced Fourier transform provided a much finer frequency resolution than the standard fast Fourier transform. The frequency resolution of the chirp z-transform is determined from the following equation.



(a) Input 1 (b) Input 2

**Figure 6.** Simulation Time History Responses to the Sum of Sine Waves Input

$$\Delta\omega_{\text{czt}} = \frac{(F_2 - F_1)}{L_w}$$

where  $(F_2 - F_1)$  determined the frequency range for the chirp-z

transform. The following chirp-z resolution was selected in order to easily maintain the frequency bookkeeping.

$$\Delta\omega_{\text{ext}} = \frac{(10.0 - 0.0)}{10000} = 0.001$$

The chirp-z transform function included in the MATLAB Signal Processing Toolbox was used to transform the time history data to the frequency domain.<sup>5</sup>

Once the data is transformed to the frequency domain, the input power spectral density, the output power spectral density, and the input-output cross spectral density were estimated from:

$$P_{xx} = \frac{|X(\omega)|^2}{N_w L_w}$$

$$P_{yy} = \frac{|Y(\omega)|^2}{N_w L_w}$$

$$P_{xy} = \frac{X^*(\omega)Y(\omega)}{N_w L_w}$$

The single input single output transfer function was then calculated from:

$$H_{ssw}(\omega) = \frac{P_{xy}(\omega)}{P_{xx}(\omega)}$$

After the transfer function was calculated, the magnitude in decibels was found from:

$$\text{mag}_{ssw} = 20\log_{10}(|H(\omega)|)$$

and the phase in degrees was found from:

$$\text{phase}_{ssw} = \frac{180}{\pi} \text{imag}(\log(H(\omega)))$$

The coherence function is a measure of how much of the output is linearly related to the input. A coherence of one indicates that all of the output is produced by the input, and a coherence of zero

indicates that none of the output is caused by the input. The coherence is calculated from the following equation.

$$C_{xy}(\omega) = \frac{|P_{xy}(\omega)|^2}{P_{xx}(\omega)P_{yy}(\omega)}$$

The frequency bookkeeping maintained when calculating the frequency responses for the concatenated data produced magnitude, phase and coherence data at 90 discrete frequencies. The data were slightly more heavily concentrated at higher frequencies than at lower frequencies. To produce data approximately evenly spaced on a logarithmic scale, 52 of the 90 discrete frequencies were selected.

#### State-space Model Fit to the Frequency Response

Once the frequency responses were calculated from the simulation data, a fourth order longitudinal state-space model was fit to the data. The four states of the model were  $u_b$ ,  $w_b$ ,  $q_b$ , and  $\theta$ ; the single input was  $\delta_e$ ; and the outputs were  $u_b$ ,  $w_b$ ,  $a_x$ ,  $a_z$ , and  $q_b$ .

The following equation is used to calculate the frequency response of a state-space model.

$$H(\omega) = C[(j\omega)I - A]^{-1}B + D$$

A cost function was set up to calculate the magnitude and phase error between the fourth order state-space model and the sum of sine waves frequency responses. The cost function was designed so that seven decibels of magnitude produced the same error as one degree of phase.<sup>6</sup>

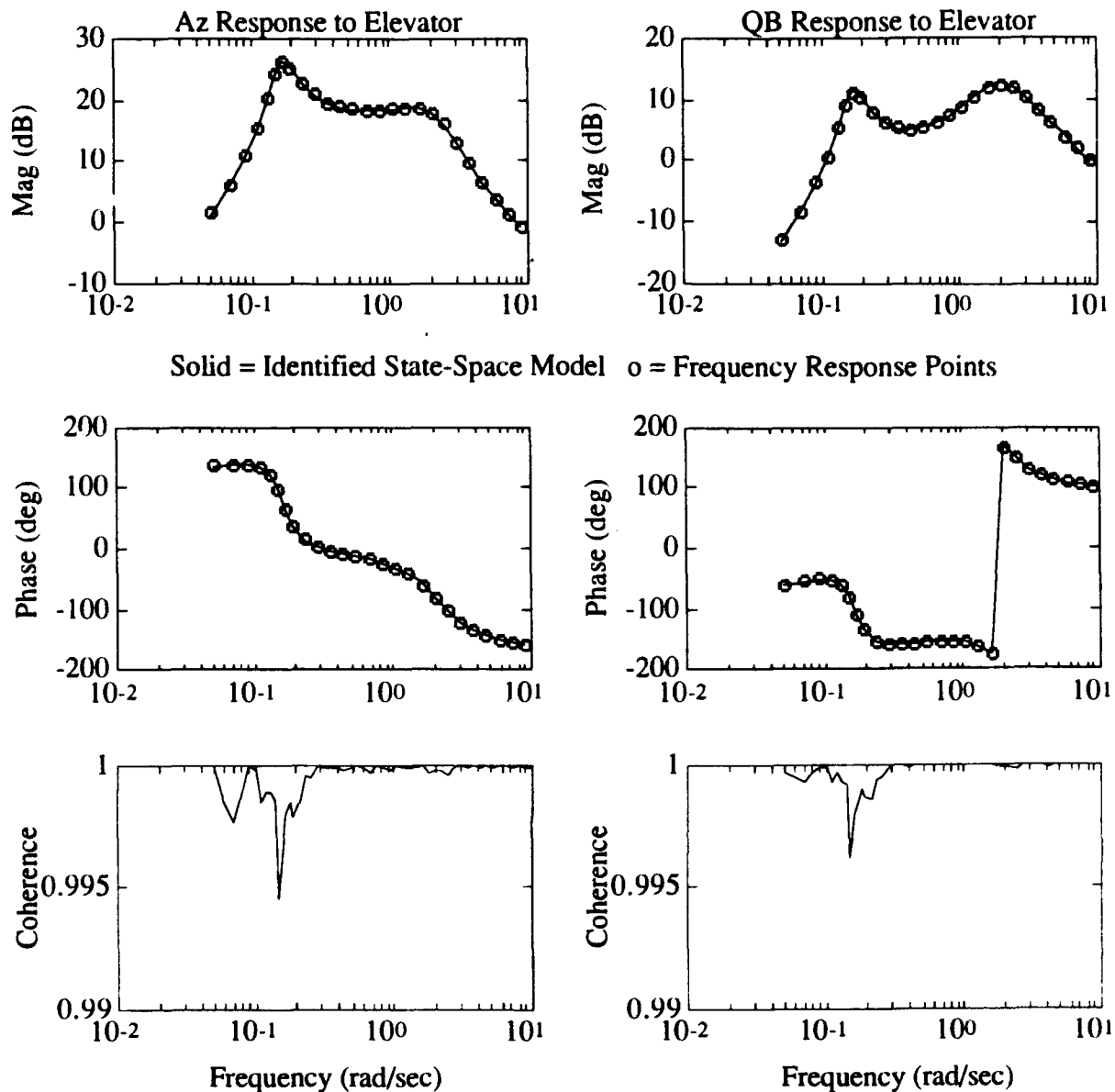


**Figure 7.** Identified Model Fit to Frequency Responses

$$\text{cost} = \sum_{i=1}^{52} (7(\text{mag}(\omega_i) - \text{mag}(\omega_i)_{\text{SSW}}))^2 + \sum_{i=1}^{52} (\text{phase}(\omega_i) - \text{phase}(\omega_i)_{\text{SSW}})^2$$

The index  $i$  is used to sum the error at each of the 52 discrete frequencies. The cost function was minimized using a binary search method called digital matching.<sup>7</sup>

The state-space model fits to the pitch rate to elevator and normal acceleration to elevator frequency responses are shown in Figure 7. Every other frequency point used in the identification was plotted for clarity. Notice the coherence for the frequency responses are very near one throughout the frequency range of interest.

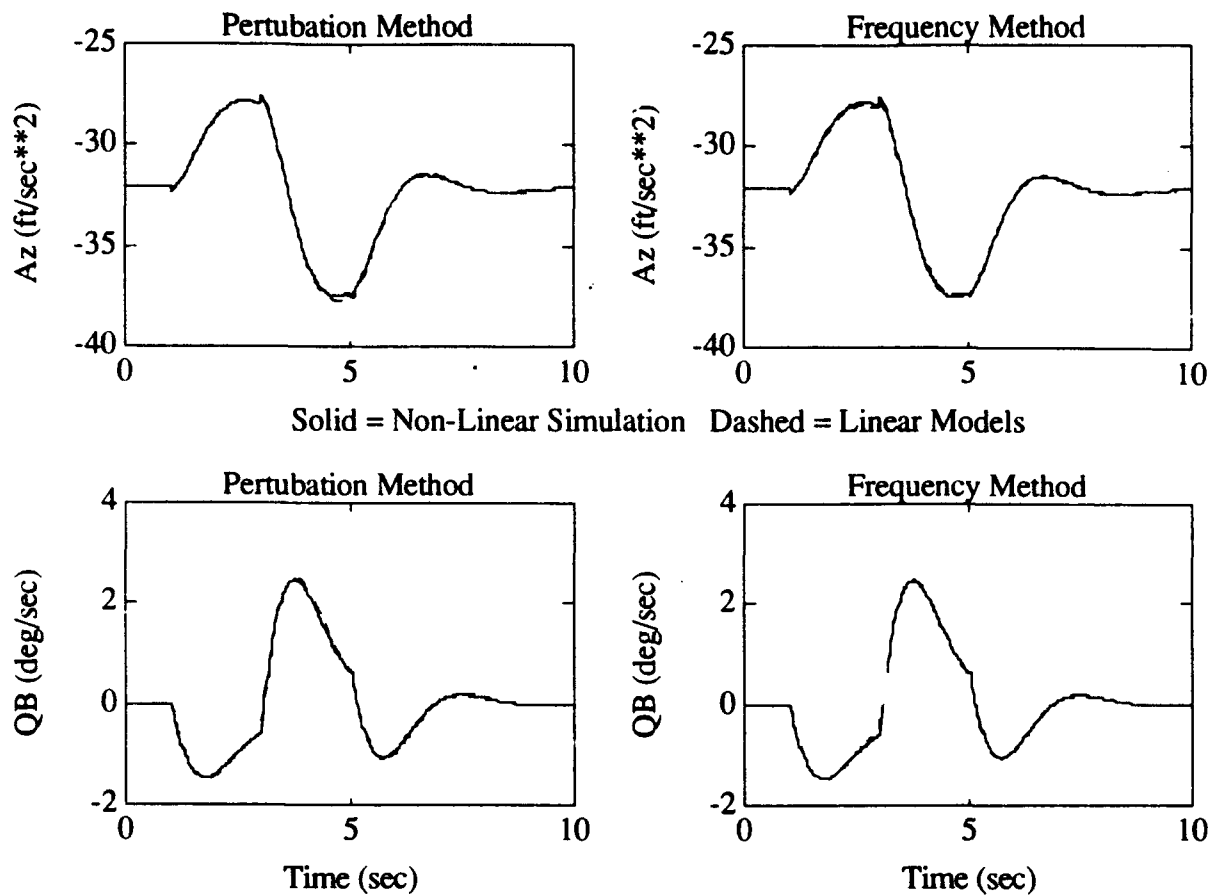


**Figure 8. Linear Model Time History Verification**

#### Model Verification

The state-space models extracted using the perturbation and frequency response methods were both verified against a time history response from the non-linear simulation. The nonlinear simulation was driven with an elevator doublet about the reference flight condition. Both linear models were then driven with the same elevator doublet. The linear model responses compared to the simulation response are shown in Figure 8.

#### Model Comparison

The short period and phugoid modes of each of the models were compared by calculating the undamped natural frequency and damping ratio of the two modes from the eigenvalues of the system matrices. Table 1 contains the undamped natural frequency and damping ratios for each method.

The frequency response was calculated from the perturbation method linear model and compared to the frequency response from the frequency method. The results are shown in Figure 9.

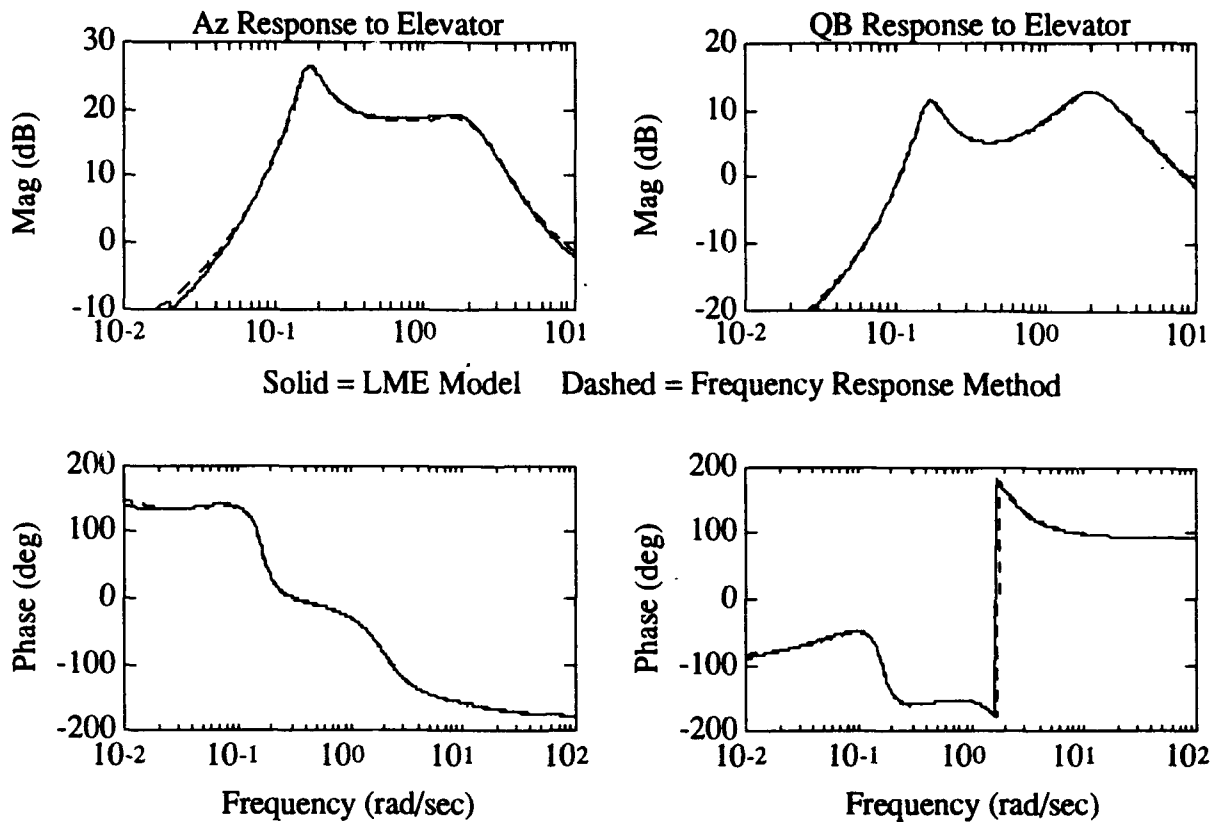


**Figure 9.** Frequency Response Comparison of Perturbation and Frequency Response Methods

	Short Period		Phugoid	
	$\omega_n$	$\zeta$	$\omega_n$	$\zeta$
perturb. method	2.01	0.497	0.165	0.192
frequency response method	2.07	0.513	0.168	0.187

**Table 1.** Undamped natural frequency and damping ratio for the short period and phugoid modes.

### Conclusions

Fourth order longitudinal state-space models were extracted from the V-22 full nonlinear simulation using the frequency response and the perturbation methods. Time history verification against the full nonlinear simulation showed that

both models accurately predicted the pitch rate and normal acceleration response to an elevator doublet. Comparison of the short period and phugoid modes, as well as the frequency response of the models, showed that similar dynamic characteristics were identified by both methods. Within the scope of this paper, both the frequency response and perturbation methods were effective means to extract a low order state-space model from a nonlinear simulation.

### Recommendations

The primary advantage to the perturbation method is that the linear model is computed directly. The frequency method requires identifying a model to fit the frequency data, which can become significantly more difficult with higher order models. When higher order models are desired, the

perturbation method offers the most direct solution.

In some cases, as in classical stability analysis of feedback loops, the frequency response is the desired end result. The perturbation method requires computing the frequency response from the linear model. Although this was a simple task for a fourth order model, computing the frequency response for very high order systems can become computationally difficult. The frequency method computes the frequency response directly and is unaffected by the order of the system. When the frequency response of large systems is desired, the frequency method should provide the most efficient solution.

6. Military Standard, "Flying Qualities of Piloted Aircraft," MIL-STD 1797, March 1987.

7. Balderson K.A., "Development of a Digital Matching Aircraft Stability Derivative Estimation Method," Masters Thesis, West Virginia University, Morgantown, WV, 1990.

### References

1. Tischler M.B., "Frequency-Response Identification of XV-15 Tilt-Rotor Aircraft Dynamics," NASA TM 89428, May 1987.

2. Schoeder J.A., Watson D.C., Tischler M.B., Eshow M.M., "Identification and Simulation Evaluation of an AH-64 Helicopter Hover Math Model," AIAA Atmospheric Flight Mechanics Conference, New Orleans, LA August 12-14 1991.

3. Ham Maj. J.A., Tischler M.B., "Flight Testing and Frequency Domain Analysis for Rotorcraft Handling Qualities Characteristics," AHS Specialists' Meeting, San Francisco, CA, January 1993.

4. Tischler M.B., Ham Maj J.A., Williams Maj. J., "Frequency Domain Testing," Class Notes, Patuxent River, MD. April 5-6 1994.

5. Krauss T.P., Shure L., Little J.N., *Signal Processing Toolbox User's Guide*, The MathWorks, Inc., Natick, Mass. 1993 pp 61-80, pp 268-269 .